Valeology: International Journal of Medical Anthropology and Bioethics (ISSN 2995-4924) VOLUME 02 ISSUE 04, 2024

SYNTHESIS AND CHARACTERIZATION OF ZnO/CdO NANOCOMPOSITE BY SOL-GEL METHOD

Samah Sabah Abdu-AL Razzaq, Alaa Jabbar Ghazai

College of Science, AL-Nahrain University, Baghdad, Iraq

Abstract:

The sol-gel approach was employed to successfully synthesise pure ZnO, CdO NPs, and ZnO/CdO nanocomposite. The purity of ZnO, CdO, and ZnO/CdO composites at different concentrations was verified using X-ray diffraction analysis. The results indicated that an increase in the CdO or ZnO ratio of the ZnO/CdO composite corresponded to an increase in the average crystal size. The FESEM pictures revealed that the predominant grain structure for pure ZnO NPs is polyhedral and tiny in size, but for pure CdO NPs, the majority of grains are spherical and big in size. The grains in ZnO/CdO nanocomposites have a spherical shape, possess a polyhedral structure, and are smaller in size compared to pure CdO nanoparticles. The lowest average particle size of the nanocomposite was 98.8 nm for the 70% ZnO/30% CdO nanocomposite. The atomic force analysis indicates that the combination of 70% ZnO/30% CdO exhibits significant values for roughness, RMS, and a small value for average grain size. The UV-VIS spectra exhibited a red shift when the CdO ratio in the nanocomposite rose. Nanocomposite materials containing zinc oxide and cadmium have several possible future uses, including photocatalysis, medicinal devices, and more. High output, great efficiency, and cheap cost are the hallmarks of this approach.

Keywords: ZnO, CdO, Sol-gel, nanocomposite.

Introduction

1. Introduction

The incredible scientific and technical progress of this century would not have been possible without nanotechnology. Recent advances in nanoscale research have opened up exciting new avenues of study in a wide variety of technological domains. Their exceptional mechanical hardness, thermal stability, chemical passivity, and enhanced optical, magnetic, electrical, and catalytic properties are the reasons behind this [1]. Zinc and cadmium oxide nanostructures are fascinating due to their n-type conductivity, making them one of the greatest materials for modern

technology. Paint colours, solar cells, and sensors are just a few of the many applications for zinc oxide and cadmium oxide [2]. In comparison to its thermal energy of 26 μeV, ZnO has a significantly higher binding energy of 60 μeV and a band gap of 3.37 eV [3]. As a semiconductor, it is known to be in the *h*-μ group of the periodic table, where ZnO is in the second group and O₂ is in the sixth. Zinc oxide was the first oxide to be used as a chemical sensor, and its sensing ability was greatly enhanced by adding cadmium oxide [4]. Concerning NO, CO, and CH4, according to what Ferro et al. [5] found. With an energy band gap of 2.3 eV and an indirect bandgap of 1.98 eV, CdO is a well-known semiconductor [6]. This aids in avoiding electron-gap recombination, which in turn lowers the band gap of zinc oxide as a result of compound development of semiconductor oxides [7], [8]. The formation of a ZnO/CdO compound is an effective technique for narrowing the energy gap [6]. This is because, as the band gap of CdO is narrower than that of ZnO, it reduces the distance between the valence band and the conduction band, which in turn facilitates electron access to the conduction band. An easy chemical method for making nanocomposite liquid material, solgel, was demonstrated in this work.

2. Experimental Work

ZnO/CdO nanocomposites were prepared using the sol-gel method. In this preparation, zinc acetate, cadmium acetate, ethanol alcohol, and mono ethanolamine were used in the following method:

Igm of zinc acetate Zn (CH3 COO)2 was taken, and 25 ml of ethanol was added. Stir it for 5 minutes, then place it on the magnetic stirrer. 8 ml of monoethanolamine is added gradually to enhance its consistency and stability. It also plays an important role in improving the strength of adhesion and drying the gel. The solution is kept in this baker on the magnetic stirrer for half an hour in order to obtain a solution homogenous, transparent, and viscous, and then heated at a temperature of 200 °C in an oven to evaporate the solvent and obtain a homogenous gelatinous substance of ZnO nanoparticles solution. The above steps are repeated, the zinc acetate is replaced with cadium acetate in the same proportion, and a solution of nanoparticles of cadium oxide is obtained. Then a ratio of 0.9 of zinc acetate and 0.1 of cadium acetate is taken, and the steps in the first paragraph are repeated to obtain the nanocomposite of ZnO/CdO. The previous process was performed with all its steps in the following properties as well: (0.8/0.2), (0.7/0.3), (0.6/0.4), (0.5/0.5) of (ZnO/CdO), (zinc acetate), and (cadmium acetate). Thus, seven preparatory samples were obtained by this method.

3. Characterization

The structural, optical, and nanostructure properties of the prepared pure ZnO, CdO NPs, and ZnO/CdO nanocomposite were studied using an XRD device using a Philips Diffractometer (40KV, Cu K α radiation with λ =1.5406Ao). Field emission scanning electron microscopy (FE-SEM, MIRA3 TESCAN) was used to analyse the structure and morphologies of the synthesised nanoparticales and nanocomposite. Image J and Origin LAB were used for statistical and image analysis. AFM (Atomic Force Microscope), the surface morphology and nanoparticle average dimension of the samples are studied by using Atomic Force Microscopy CSPM AA3000 AFM supplied by Angstrom Company. Ultraviolet spectroscopy was used to observe the optical absorption of the ZnO-CdO nanocomposite using a Shimazu spectrometer (2000) in the range of 200–1100 nm.

4. Result and Discussion

4.1. X-ray diffraction spectra

Zinc oxide, cadmium oxide, and their compounds' structural characteristics may be understood from the X-ray spectrum pattern. In order to match the samples, we employed the x-pert software, and to estimate their crystal size, we used the Scherer equation [9]:

$$C.S. = \frac{K \lambda}{(FWHM) \cos \theta}$$

In this formula, K is the shape factor, λ is the X-ray radiation's wavelength, (FWHM) is the diffraction peak's full width at half maximum (in radians), and θ is the diffraction angle of Bragg's diffraction peak.

The X-ray diffraction patterns of pure ZnO and CdO as well as ZnO/CdO composites at varying concentrations are shown in Figure 1. As an additional item, we have the JCPDS for the CdO card (01-075-0591) and the ZnO card (01-080-0075). Table 1 provides useful information on the crystal size, peak positions, Miller indices for diffracting planes, and full width at half maximum (FWHM) for the three diffraction peaks of ZnO and CdO materials, as well as the patterns of diffraction peaks. The results show that CdO has a cubic crystal structure and ZnO a hexagonal one. Other materials do not show any diffraction peaks, suggesting that the phase in question is clear of contaminants. The diffraction peaks of CdO and ZnO become more intense when the ZnO or CdO ratio in the ZnO/CdO composite rises, as seen in Figure 1. The ZnO/CdO composite shows no phase shift and no additional diffraction peaks for either component. Table 1 shows that as the ZnO/CdO composite's CdO or ZnO ratio increases, the average crystal size also increases. These results are consistent with the results obtained in reference [10], [11].

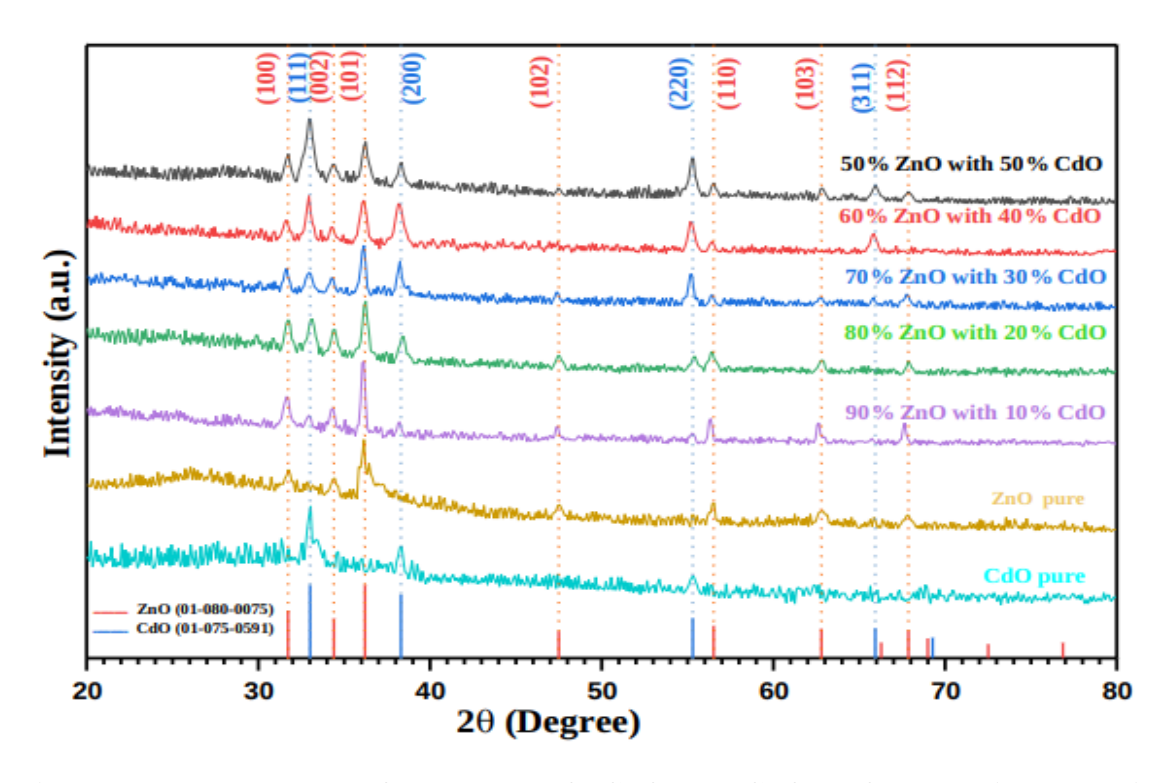


Figure 1: XRD spectrum of the pure ZnO, CdO, and CdO-ZnO composite at varying concentrations

Table 1: XRD analysis of ZnO, CdO pure, and ZnO/CdO composite with different concentrations of ZnO and CdO

Sample		2? (deg)	FWHM (deg)	dexp (A)	D (nm)	D _{Avg} (nm)	2? (deg)	d:n (A)	hkl	No. card	Structure
ZnO		31.72	0.5904	2.821	14.6	21.95	31.728	2.818	100	01-079-0208	Hexagonal
		34.44	0.2952	2.604	29.4		34.4	2.605	002		
		36.04	0.2952	2.492	29.6		36.212	2.479	101		mal
CdO		32.96	0.2952	2.717	29.3	24.89	33.02	2.711	111	01-075-0591	Cubic
		38.26	0.2952	2.352	29.8		38.313	2.347	200		
		55.32	0.6	1.659	15.6		55.3	1.66	220		
	for Zn O	31.57	0.5793	2.826	14.9	27.25	31.728	2.818	100	01-079-0208	Hexagonal
9		34.32	0.2952	2.607	29.4		34.4	2.605	002		
90% ZnO with 10% CdO		36.11	0.2952	2.488	29.6		36.212	2.479	101		
	for Cd O	32.93	0.5288	2.71	16.4	18.09	33.02	2.711	111	01-075-0591	Cubic
		38.2	0.5718	2.346	15.4		38.313	2.347	200		
		55.21	0.4152	1.66	22.6		55.3	1.66	220		
	for Zn O	31.72	0.5514	2.821	15.6	20.92	31.728	2.818	100	01-079-0208	Ħ
80 % Zn O with 20% CdO		34.42	0.5086	2.606	17.1		34.4	2.605	002		Hexagonal
		36.18	0.4113	2.483	21.2		36.212	2.479	101		onal
	for Cd O	33.09	0.7382	2.707	11.7	17.22	33.02	2.711	111	01-075-0591	
		38.41	0.4205	2.344	20.9		38.313	2.347	200		Cubic
		55.4	0.492	1.658	19		55.3	1.66	220		ic
	for Zn O	31.72	0.5514	2.821	15.6	20.92	31.728	2.818	100	01-079-0208	H
8		34.42	0.5086	2.606	17.1		34.4	2.605	002		Hexagonal
70%ZnO with 30% CdO		36.18	0.4113	2.483	21.2		36.212	2.479	101		nal
	for Cd O	32.93	0.5587	2.71	15.5	22.66	33.02	2.711	111	01-075-0591	Cubic
O III		38.23	0.3198	2.348	27.5		38.313	2.347	200		
		55,22	0.6581	1.658	14.2		55.3	1.66	220		ic
	for Zn O	31.68	0.5043	2.824	17.1	18.99	31.728	2.818	100	01-079-0208	Hexagonal
8		34.34	0.4593	2.611	18.9		34.4	2.605	002		
60%ZnO with 40%CdO		36.13	0.4593	2.486	19		36.212	2.479	101		
%ZnO wi 40%CdO	for Cd O	32.93	0.5147	2.72	16.8	20.89	33.02	2.711	111	01-075-0591	П
vith		38.18	0.492	2.357	17.8		38.313	2.347	200		Cubic
		55.21	0.3936	1.664	23.8		55.3	1.66	220		ic
	for Zn O	31.7	0.5436	2.823	15.9	23.36	31.619	2.827	100	01-079-0208	Hexagonal
50%ZnO with 50% CdO		34.39	0.6114	2.608	14.2		34.335	2.61	002		
		36.24	0.512	2.479	17.1		36.1	2.486	101	0208	onal
%ZnO wi 50% CdO	for Cd O	32.98	0.5513	2.716	15.7	21.22	33.02	2.711	111		
Owith		38.27	0.4695	2.352	18.7		38.313	2.347	200	01-075-0591	Cubic
		55,35	0.3698	1.66	25.3		55.3	1.66	220		vic
						L				_	

3.2. Field Emission Scanning Electron Microscope (FESEM)

After preparing the pure ZnO, CdO nanoparticles, and the ZnO/CdO nanocomposite in liquid form, they were deposited on glass substrate by the casting method, treated at a temperature of 200 °C to get rid of solvents, obtain a thin film for all samples, and examined with a Field Emission Scanning Electron Microscope (FESEM).

The FE-SEM image in Figures 2–8 shows pure ZnO, CdO nanoparticales (NPs), and ZnO/CdO nanocomposite with different percentages of wt%. Figure 2 revealed that ZnO NPs had a morphology that was primarily polyhedron grains and dumbbell-shaped, with an average particle size of 69.7 nm, as shown in figure 2a. However, the majority of nanoparticales diameter values range almost between 20 and 165 nm, as shown in figure 2b.

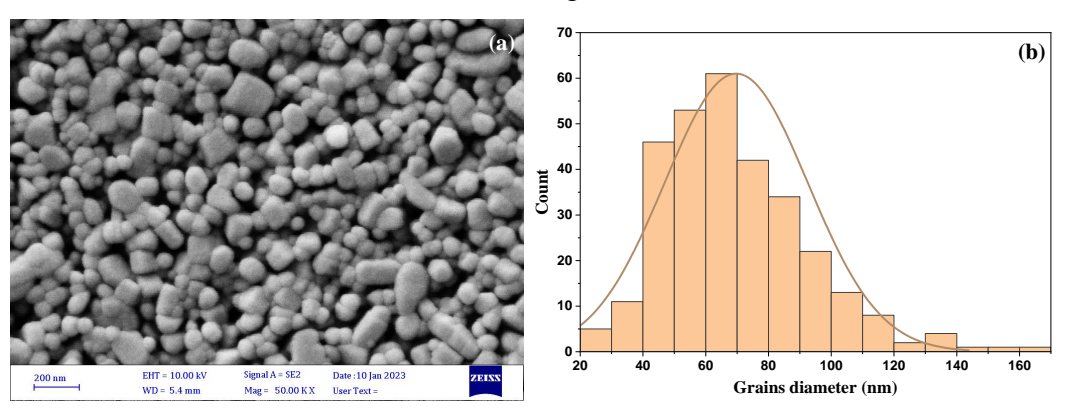


Figure 2: The FE-SEM image of (a) pure ZnO nanoparticales with magnification of 50KX, (b) Histograms of diameters with Gaussian distribution.

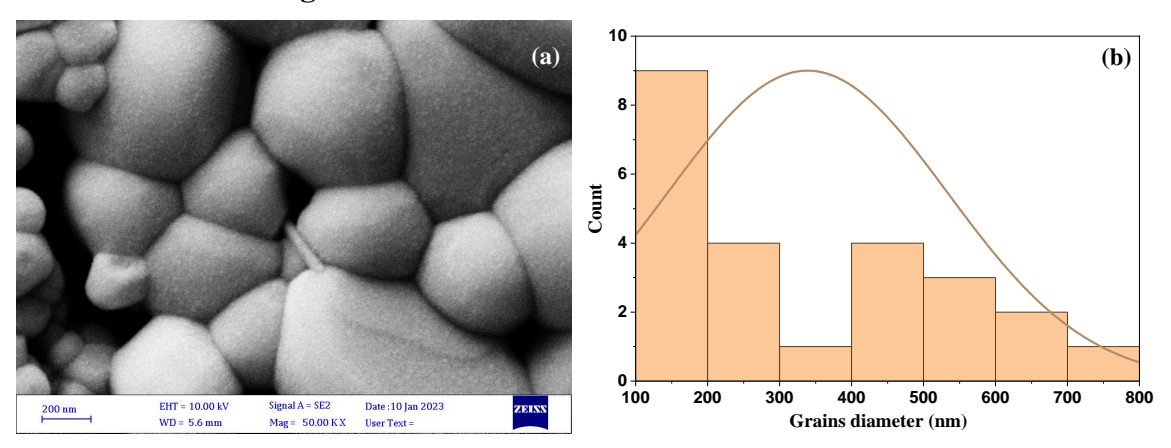


Figure 3: The FE-SEM image of (a) pure CdO nanoparticales with magnification of 50KX, (b) Histograms of diameters with Gaussian distribution.

As for the CdO nanoparticles, their sizes are larger; their average size is 338 nm, and they have a spherical shape and polyhedron grains, as shown in figure 3a. Based on the diameter distribution histograms, the statistical results show that most values of the nanoparticles diameter range almost from 100 nm to less than 800 nm, as shown in figure 3b.

The ZnO/CdO nanocomposites shown in Figures 4–8 show that as the amount of CdO in the nanocomposite rises, the grains get smaller compared to pure CdO. At 70% ZnO/30% CdO, the average diameter of the grains is 98.8 nm. Then, when the ratio of CdO in the nanocomposite increases, the grain sizes increase, so that the average grain diameter is 217.9 nm at the ratio of 50% ZnO/50% CdO nanocomposite.

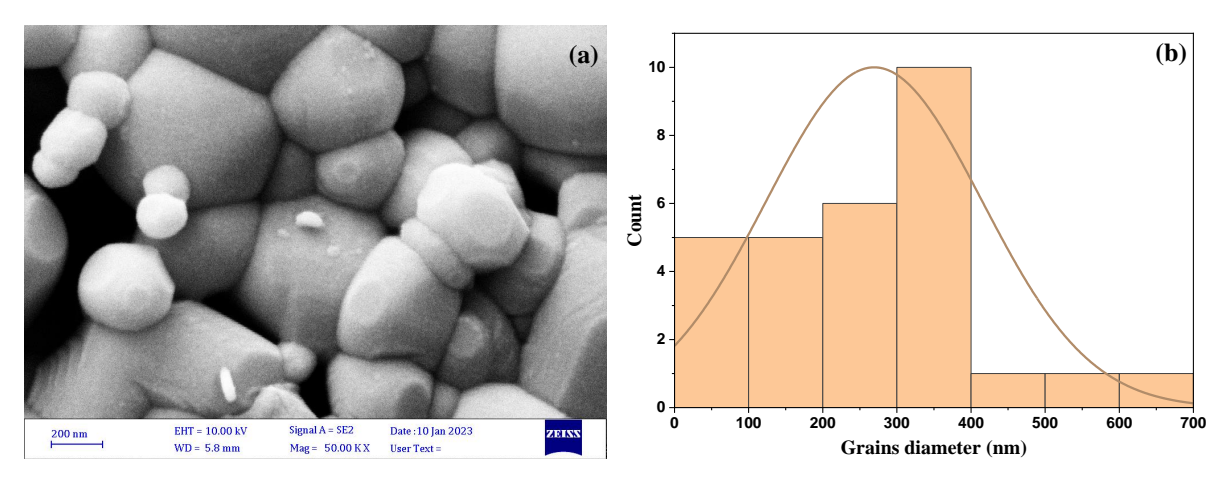


Figure 4: The FE-SEM image of (a) 90% ZnO/10% CdO nanocomposite with magnification of 50KX, (b) Histograms of diameters with Gaussian distribution.

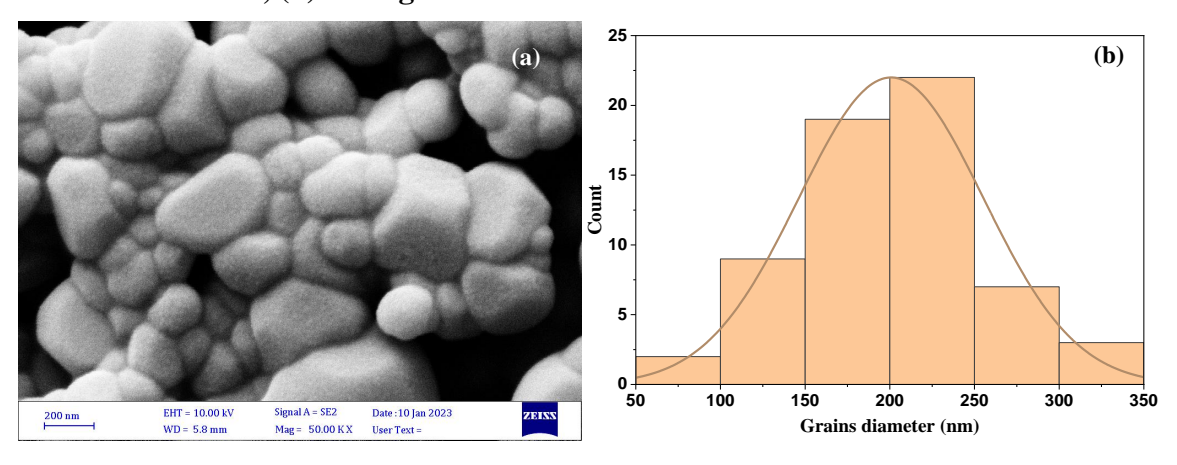


Figure 5: The FE-SEM image of (a) 80% ZnO/20% CdO nanocomposite with magnification of 50KX, (b) Histograms of diameters with Gaussian distribution.

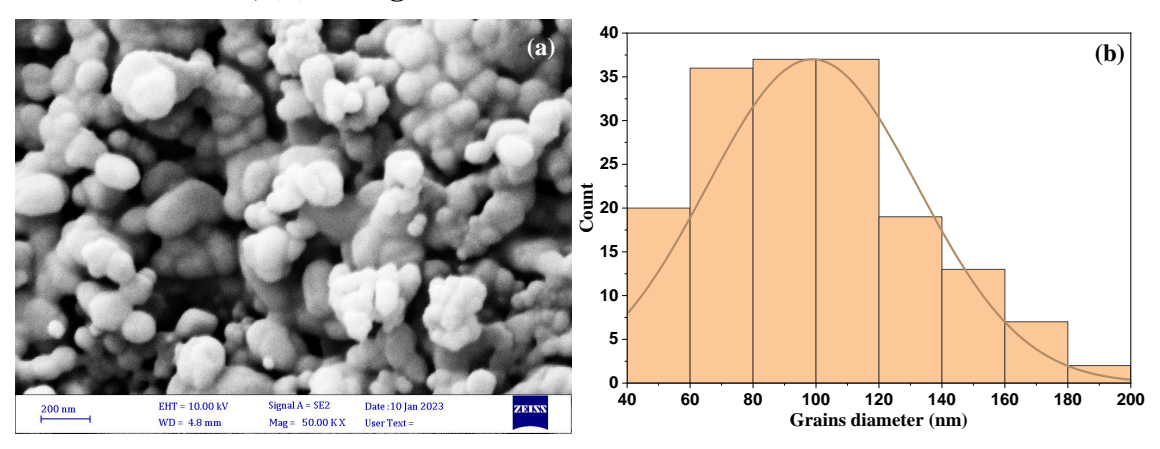


Figure 6: The FE-SEM image of (a) 70% ZnO/30% CdO nanocomposite with magnification of 50KX, (b) Histograms of diameters with Gaussian distribution.

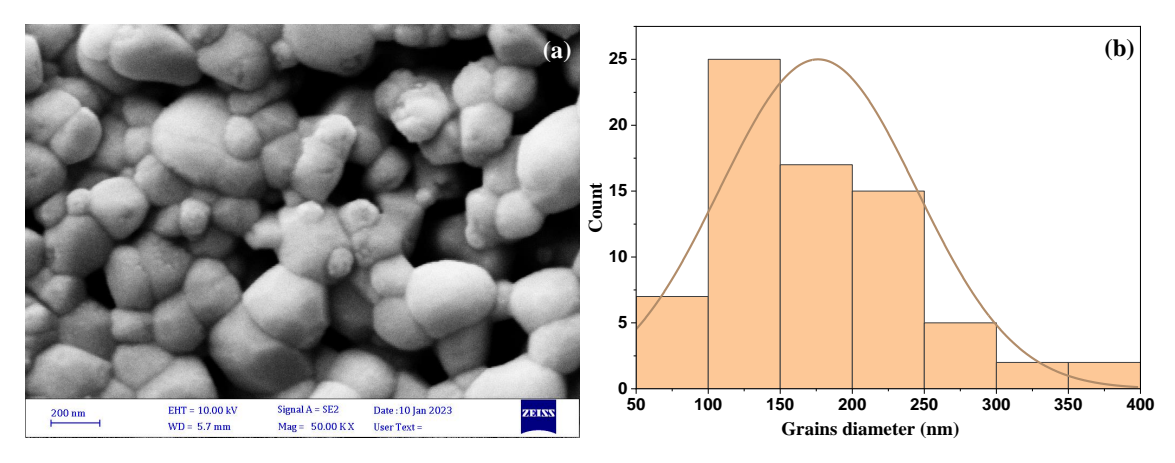


Figure 7: The FE-SEM image of (a) 60% ZnO/40% CdO nanocomposite with magnification of 50KX, (b) Histograms of diameters with Gaussian distribution.

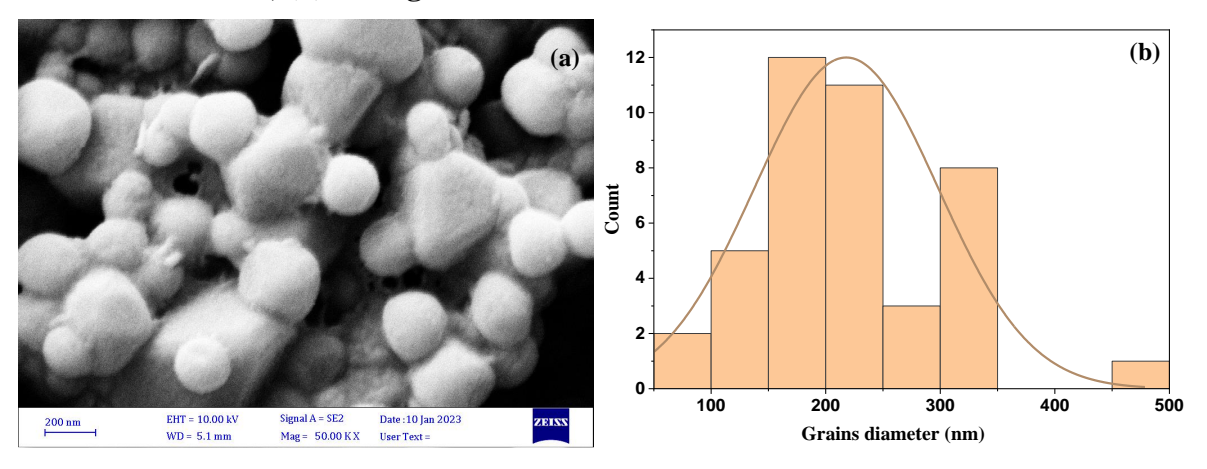


Figure 8: The FE-SEM image of (a) 50% ZnO/50% CdO nanocomposite with magnification of 50KX, (b) Histograms of diameters with Gaussian distribution.

The observed morphology was a result of combining both oxide morphologies, as follows: The morphology of the majority of the grains is polyhedral, and a few of them have a spherical shape at the ratio of 90% ZnO/10% CdO, while the spherical shape of the grains increases with the increase in the ratio of CdO in the nanocomposite, and the ratio of polyhedral granules decreases. The vibrant hue observed in the images can be attributed to the phenomenon of particle charging upon exposure to electron light [10].

3.3. Atomic force analysis

Figure 9 displays a three-dimensional atomic force microscopy (AFM) picture depicting the surface structure of the pure ZnO, CdO, and ZnO/CdO nanocomposite at various concentrations of ZnO and CdO. The pellet surface of all samples exhibits uniform granules that are vertically cut into a spherical shape, accompanied by well-defined coarse grains inside the scanning region of 2.5x2.5 μm. Table 2 presents the computed and recorded root mean square (RMS) values for surface rate, roughness, and average particle size. The findings shown in Table 2 and Figure 9 indicate that the combination of 70% ZnO/30% CdO exhibits significant values for roughness, average grain size, and RMS. The AFM results exhibit a high degree of concurrence with the findings of X-ray diffraction and FEMSE analysis.

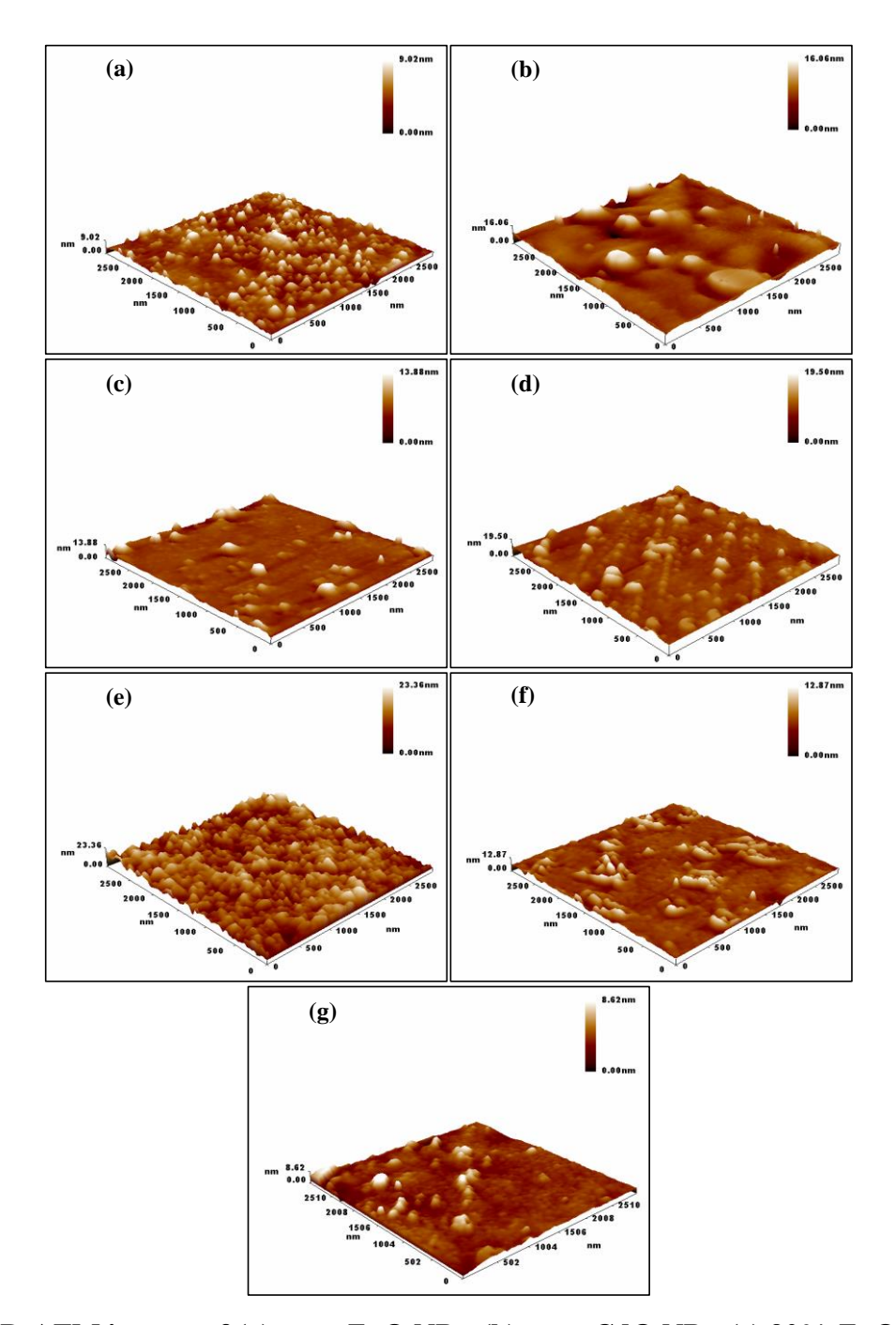


Figure 9: 3D-AFM images of (a) pure ZnO NPs, (b) pure CdO NPs, (c) 90% ZnO/10% CdO nanocomposite, (d) 80% ZnO/20% CdO nanocomposite, (e) 70% ZnO/30% CdO nanocomposite, (f) 60% ZnO/40% CdO nanocomposite, and (g) 50% ZnO/50% CdO nanocomposite.

Table 2: AFM analysis of pure ZnO, CdO NPs, and ZnO/CdO nanocomposite with different concentrations of ZnO and CdO.

sample	Roughness (nm)	Avg Diameter (nm)	RMS (nm)
Pure ZnO NPs	0.788	119.33	1.09
Pure CdO NPs	1.39	160.49	2
90%ZnO/10%CdO nanocomposite	0.618	140.73	1.12
80%ZnO/20%CdO nanocomposite	0.96	128.45	1.42

70%ZnO/30%CdO nanocomposite	2.52	119.54	3.14
60%ZnO/40%CdO nanocomposite	0.853	130.51	1.29
50%ZnO/50%CdO nanocomposite	0.606	122.09	0.943

3.4. Optical Properties

Figure 10 displays the UV-VIS spectra, which measure the absorbance of the ZnO, CdO pure, and ZnO/CdO nanocomposite from 300 to 900 nm, for different concentrations of ZnO and CdO. All of the synthetic materials, including CdO and ZnO, absorb light in the ultraviolet and visible spectrums. By increasing the concentration of CdO in the ZnO/CdO nanocomposite, the absorbance rises and the red shift deepens [12]. This is because surface optical scattering of incoming light becomes more noticeable. In comparison to the 387 nm and 513 nm optical absorption spectra of pure ZnO and CdO, respectively, the absorption edge of a CdO/ZnO nanocomposite with varied concentrations ranges from 390 to 434 nm. The visible region may be utilised to respond to the ZnO by mixing it with CdO nanoparticles, as shown by the absorption edge of the CdO/ZnO nanocomposite, which is similar to a pattern observed in the literature [13].

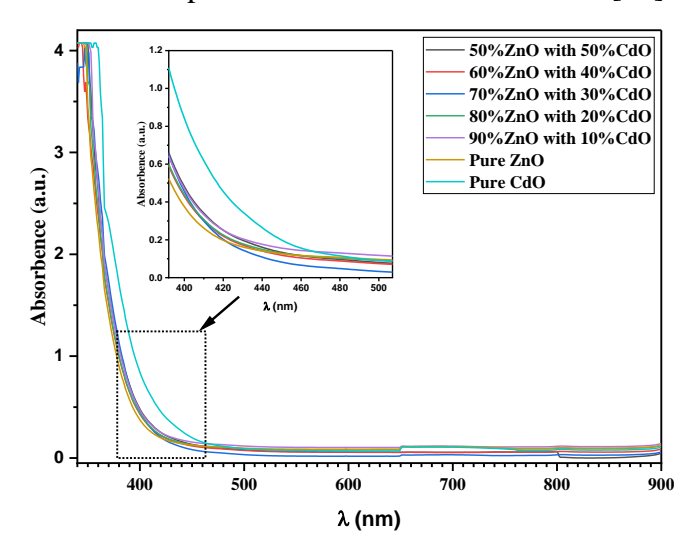


Figure 10: Absorbance of ZnO, CdO pure and different wight of ZnO-CdO nanocomposite at varying concentrations.

Conclusion

Pure ZnO, CdO NPs, and ZnO/CdO nanocomposite were successfully synthesized through the solgel method. X-ray diffraction confirmed the purity of ZnO, CdO, and ZnO/CdO composites at varying concentrations and showed that as the ZnO/CdO composite's CdO or ZnO ratio increases, the average crystal size also increases. FESEM images showed that the majority of the grains are polyhedral and small in size for pure ZnO NPs, while the majority are spherical and large in size for pure CdO NPs. For ZnO/CdO nanocomposites, the grains are spherical, polyhedral, and smaller in size than for pure CdO NPs. UV-VIS spectra showed that when the ratio of CdO in the nanocomposite increased, there was a red shift. ZnO/CdO nanocomposite offer great potential in future application for many devices and can be used in photocatalysis medical device, and other application. This method is characterized by high production, high efficiency, and lower cost.

Reference

- 1. M. Lashanizadegan, "Synthesis of Cd (OH) 2 and CdO nanoparticles via a PEG-assisted route," *J. Ceram. Process. Res.*, vol. 13, no. 4, pp. 389–391, 2012.
- 2. K. Kalpanadevi, C. R. Sinduja, and R. Manimekalai, "Characterisation of zinc oxide and cadmium oxide nanostructures obtained from the low temperature thermal decomposition of

- inorganic precursors," Int. Sch. Res. Not., vol. 2013, 2013.
- 3. G. Xiong, U. Pal, J. G. Serrano, K. B. Ucer, and R. T. Williams, "Photoluminesence and FTIR study of ZnO nanoparticles: the impurity and defect perspective," *Phys. status solidi c*, vol. 3, no. 10, pp. 3577–3581, 2006.
- 4. H. Karami, "Investigation of sol-gel synthesized CdO-ZnO nanocomposite for CO gas sensing," *Int. J. Electrochem. Sci.*, vol. 5, no. 5, pp. 720–730, 2010.
- 5. G. E. Patil, D. D. Kajale, V. B. Gaikwad, and G. H. Jain, "Preparation and characterization of SnO2 nanoparticles by hydrothermal route," *Int. Nano Lett.*, vol. 2, no. 1, p. 17, 2012.
- 6. A. Tadjarodi and M. Imani, "Synthesis and characterization of CdO nanocrystalline structure by mechanochemical method," *Mater. Lett.*, vol. 65, no. 6, pp. 1025–1027, 2011.
- 7. R. Saravanan, H. Shankar, T. Prakash, V. Narayanan, and A. Stephen, "ZnO/CdO composite nanorods for photocatalytic degradation of methylene blue under visible light," *Mater. Chem. Phys.*, vol. 125, no. 1–2, pp. 277–280, 2011.
- 8. S. Balachandran, S. G. Praveen, R. Velmurugan, and M. Swaminathan, "Facile fabrication of highly efficient, reusable heterostructured Ag–ZnO–CdO and its twin applications of dye degradation under natural sunlight and self-cleaning," *Rsc Adv.*, vol. 4, no. 9, pp. 4353–4362, 2014.
- 9. N. K. Hassan, M. R. Hashim, and N. K. Allam, "A facile room temperature electrochemical deposition of pyramidal ZnO nanostructures: Suppressing the green emission," *Phys. E Low-dimensional Syst. Nanostructures*, vol. 44, no. 9, pp. 1853–1856, 2012.
- 10. N. Sahu and R. K. Duchaniya, "Synthesis of ZnO-CdO Nanocomposites," *J. Mater. Sci. Surf. Eng.*, vol. 1, no. 1, pp. 11–14, 2013.
- 11. Z. Tian, Y. Chen, W. Yang, J. Yao, L. Zhu, and Z. Shuai, "Low-dimensional aggregates from stilbazolium-like dyes," *Angew. Chemie Int. Ed.*, vol. 43, no. 31, pp. 4060–4063, 2004.
- 12. R. A. Zargar, A. H. Shah, M. Arora, and F. A. Mir, "Crystallographic, spectroscopic and electrical study of ZnO: CdO nanocomposite-coated films for photovoltaic applications," *Arab. J. Sci. Eng.*, vol. 44, no. 7, pp. 6631–6636, 2019.
- 13. C. V. Reddy, B. Babu, and J. Shim, "Synthesis, optical properties and efficient photocatalytic activity of CdO/ZnO hybrid nanocomposite," *J. Phys. Chem. Solids*, vol. 112, pp. 20–28, 2018.